

Drilling reveals fluid control on architecture and rupture of the Alpine Fault, New Zealand

R. Sutherland¹, V.G. Toy², J. Townend³, S.C. Cox⁴, J.D. Eccles⁵, D.R. Faulkner⁶, D.J. Prior^{2,6}, R.J. Norris², E. Mariani⁶, C. Boulton⁷, B.M. Carpenter⁸, C.D. Menzies⁹, T.A. Little³, M. Hasting⁵, G.P. De Pascale⁷, R.M. Langridge¹, H.R. Scott², Z. Reid-Lindroos², B. Fleming², A.J. Kopf¹⁰

¹ GNS Science, PO Box 30368, Lower Hutt 5040, New Zealand

² University of Otago, PO Box 56, Dunedin, New Zealand

³ Victoria University of Wellington, PO Box 600, Wellington, New Zealand

⁴ GNS Science, Private Bag 1930, Dunedin 9054, New Zealand

⁵ IESE, University of Auckland, Private Bag 92019, Auckland, New Zealand

⁶ University of Liverpool, Merseyside L69 3GP, England

⁷ University of Canterbury, Private Bag 4800, Christchurch 8140, New Zealand

⁸ Istituto Nazionale di Geofisica e Vulcanologia, Rome 00143, Italy

⁹ University of Southampton, Southampton, SO14 3ZH, England

¹⁰ MARUM, University of Bremen, PO Box 330440, 28344 Bremen, Germany

Supplementary Material

Contents

Deep Fault Drilling Project (DFDP), Alpine Fault.....	2
Fault geometry and overview of rock units	3
Quaternary gravel.....	3
Hanging-wall ultramylonite	3
Hanging-wall cataclasite.....	4
Fault gouge and ultracataclasite (includes active PSZ)	5
Footwall cataclasite.....	5
Fluid pressures, temperatures, and hydraulic observations	6
ACKNOWLEDGMENTS	6
Figures.....	7
Figure S1. Wireline geophysical data obtained in DFDP-1B	7
Figure S2. Pressure decline data from (A) slug tests; and (B) post-completion.....	8
References.....	9

Deep Fault Drilling Project (DFDP), Alpine Fault

Understanding the conditions that prevail within the interiors of active faults is crucial for elucidating mechanisms governing long-term fault evolution and, in particular, the earthquake-rupture processes that are of special interest to society (Tullis et al., 2007; Zoback et al., 2007).

The DFDP project is a multi-phase experiment that will eventually drill to depths sufficient to characterize and see through thermal, hydrological, and stress perturbations associated with topographic relief near the Alpine Fault, and to thus make and test predictions of ambient conditions in the seismogenic mid-crust (Townend et al., 2009). The staged approach to rock sampling and measurement at progressively greater depths will track the evolution of processes and overprints that operate on the fault along a single exhumation pathway. In contrast to drilling studies of recently ruptured faults (Fujimoto et al., 2007; Wang et al., 2005), DFDP aims to investigate a mature plate-bounding fault that has a high probability of rupture in a large earthquake during coming decades.

At least nine key attributes make the central Alpine Fault an attractive target:

- 1) Well-determined and rapid (c. 26 mm/yr) Pleistocene slip rates (Norris and Cooper, 2001; Sutherland et al., 2006);
- 2) Precisely known plate motion history with a single fault that has accommodated most plate boundary displacement for >20 Myr (Cande and Stock, 2004; DeMets et al., 2010; Sutherland, 1999; Sutherland et al., 2000); MORVEL-1 plate motion at the drilling site (Fig. 1C) is 39.8 ± 0.7 mm/yr towards $245.5 \pm 0.9^\circ$ (DeMets et al., 2010).
- 3) More than 300 km of along-strike exposure of uniform-composition rocks in the hanging wall and fault rocks derived from them (Cooper and Norris, 2011);
- 4) Sequences of fault rocks developed during unidirectional exhumation on well-determined trajectories over relatively short time periods (Little et al., 2005; Norris and Cooper, 2007);
- 5) Rapid uplift resulting in advection of crustal isotherms in the hangingwall so that brittle-ductile transition processes can be studied at shallower (potentially drillable) depths than normal (Allis and Shi, 1995; Holm et al., 1989; Koons, 1987; Toy et al., 2010);
- 6) The opportunity to monitor a locked fault late in its earthquake cycle with a high (c. 15-32%) probability of rupture in the lifetime of a fault-zone observatory (c. 30 years) (Rhoades and Van Dissen, 2003) ;
- 7) An extensive body of existing geological and geophysical knowledge, and a modern nationwide geophysical monitoring network ('GeoNet');
- 8) An inclined fault orientation enabling fault penetration with sub-vertical boreholes (Norris et al., 1990); and
- 9) A relatively benign political and physical environment in which to operate, with existing industry and supporting infrastructure.

The DFDP project completed Phase 1 by drilling two boreholes at Gaunt Creek, c. 20 km northeast of Franz Josef Glacier (Cooper and Norris, 1994) during January and February 2011. Two vertical boreholes (<2° deviation) were drilled to depths of 100.6 m (DFDP-1A) and 151.4

m (DFDP-1B). The DFDP-1 phase yielded the first continuous set of rock cores and wireline logs through the Alpine Fault, enabled hydraulic observations to be made, and established long-term monitoring of temperatures, fluid pressures and chemistry, and seismic activity near the fault.

We advanced 150 mm steel casing using a downhole pneumatic hammer system to establish each borehole. We then used a PQ3 diamond coring system with water-based mud to recover 86 mm diameter rock cores. Wireline geophysical tools were run downhole immediately after drilling, and then observatory sensors were installed. Slug tests were conducted at a number of breaks during each phase. A full description of drilling and other operational procedures, core handling, wireline tools, and other instrumentation is given in a full borehole completion report (Sutherland et al., 2011).

Fault geometry and overview of rock units

DFDP-1 results confirm that the Alpine Fault at Gaunt Creek dips southeast at c. 30–39°, except in its shallowest part where it is subhorizontal (Fig. 1). We recognise four main lithological units in the subsurface on the basis of macroscopic brittle structures and mineralogy, in addition to Quaternary gravel units (Fig. 1). The PSZ can be identified offsetting gouge against gravel on either side of Gaunt Creek valley and is clear in both DFDP-1 boreholes. Late Quaternary displacements of 180 m and 110 m measured from outcrop of a discrete surface emplacing cataclasite above gravel imply a local slip rate on the PSZ of $>21 \pm 3$ mm/yr (Cooper and Norris, 1994).

Quaternary gravel

Gravel 1, which occurs at the base of borehole DFDP-1A, is composed primarily of Alpine Schist clasts and is interpreted as a coarse fluvial deposit. The top of this unit is correlated with basal gravel observed in nearby surface outcrops (Fig. 1), which is inferred to have been deposited during the main phase of most recent deglaciation that started at 19.5–18.3 ka calBP (Almond et al., 2001; Vandergoes and Fitzsimons, 2003).

Gravel 2 (Fig. 1B) is a talus deposit stratigraphically overlying Gravel 1 in outcrop and composed of angular mylonite clasts. Erosion of the overthrust fault rock wedge is interpreted to have formed a free ground surface that was buried as this wedge was thrust over it. Gravel 2 has been dated as 15.0 ka calBP (Cooper and Norris, 1994). This unit is overlain by fluvial deposits dated as 12.1 ka calBP that have correlatives in the hanging-wall and accommodation of the significant displacement requires localisation of strain near the surface on a very narrow zone (<1 m) since their deposition (Cooper and Norris, 1994).

Gravel 3 comprises reworked landslide or debris flow deposits incised by degradational terraces. The trace of the Alpine Fault does not offset these terraces, so surface relief likely postdates 1717 AD. Gravel 4 is the active river bed of Gaunt Creek.

Hanging-wall ultramylonite

DFDP-1A and DFDP-1B both sampled the hanging-wall of the Alpine Fault within c. 100 m of the PSZ, where it is composed of ultramylonitic fault rocks exhibiting a planar foliation formed during ductile shearing at temperatures exceeding that of the brittle-creep transition at c. 300°C (Norris and Cooper, 2007; Toy et al., 2008). They are variably black to dark grey or dark green,

changing to brown, green and black downwards. Quartz segregation laminae commonly delineate a mm-spaced foliation and trains of mm-diameter feldspar augen are locally present. The most common protolith is inferred to be hanging-wall amphibolite-facies Alpine Schist of quartzofeldspathic to metabasic composition (Cooper and Norris, 2011). Ultramylonites in DFDP-1 core display pervasive cataclastic overprints in <1 m-thick zones, an early generation of which commonly were cemented and then refractured.

Low-displacement mm- to cm-spaced fractures are pervasive throughout the Alpine Fault ultramylonite zone (Norris and Cooper, 2007); these posed significant borehole stability and core recovery challenges. The fractures are generally open and exhibit very little coating (some clay may have washed away during drilling), but rare clays are preserved along localised secondary faults close to the PSZ. In outcrop, mm-thick uncemented layers of clays and rare quartz veins are visible along fractures.

Neutron logs from the upper part of the DFDP-1B borehole (depth 50–65 m) yield apparent porosity values of 2–10%; these values increase downwards but are significantly affected by borehole enlargement recorded by caliper logs and may also reflect clay-bound water rather than macroscopic pore fluids. An increase in the natural gamma radiation signal downward in this unit is consistent with greater K^+ towards the base of both boreholes. Spontaneous potential values increase systematically with depth from 140 to 240 mV in the basal 50 m of the unit, reflecting greater membrane potentials caused by greater clay abundance. Density, resistivity, and spontaneous potential data are also consistent with an increase in the concentration of fractures and clay closer to the PSZ (Fig. DR1). Typical guard-determined resistivity values are 300–500 Ω m in DFDP-1B, reducing downward to values as low as 100–150 Ω m near the base of the mylonite zone. A sharp boundary at the base of this unit is observed in spontaneous potential and neutron porosity logs at 100 m depth in DFDP-1B (Fig. 2).

Hanging-wall cataclasite

Within c. 20 m of the PSZ, we collected near-perfect core samples that record a progressive downwards transition from ultramylonite to paler green cataclasite that is cemented, cohesive, and foliated in places (Fig. 1). In some cases the foliation is a remnant of the parent mylonite; in others it is a newly-developed cleavage defined by anastomosing clay or phyllosilicate-rich layers and shear fractures (mode II-III). Outcrop samples of the same unit show it is composed of variably shattered ultramylonite that has been extensively altered so that it now contains the minerals chlorite, illite-muscovite, biotite, smectite, vermiculite, and is cemented by carbonate (Warr and Cox, 2001).

Compensated density logs yield a value of 2.4 ± 0.1 g cm⁻³ for most of the hanging-wall cataclasite in both boreholes (Fig. DR1). Sonic velocity increases abruptly downward across the contact between ultramylonite and cataclasite. Spontaneous potential progressively increases downwards through the cataclasite from 200 mV to 230 mV in DFDP-1B. Resistivity decreases downward in DFDP-1B from c. 275 Ω m to c. 125 Ω m. The lower electrical resistivity of the cataclasite than overlying ultramylonite is likely due to the availability of ions on interconnected hydrous clay surfaces. Neutron porosity values are 1–15% in DFDP-1A and increase downward from c. 2% to c. 15% in DFDP-1B.

Fault gouge and ultracataclasite (includes active PSZ)

The central part of the fault zone consists of ultracataclasite and gouge that form a narrow, discrete, ultrafine-grained, brownish-grey interval with very high clay concentration. In DFDP-1A, this material, of which we sampled a 0.2 m thick interval in the centre of an unbroken core, also demarcates the contact between cataclasite and Quaternary gravel; thus we interpret this gouge as the principal slip zone (PSZ). Wireline logs record resistivity values of $<100 \Omega \text{ m}$ in the 0.3 m above the gravel contact, and values lower than in any other part of the borehole ($<200 \Omega \text{ m}$) in the zone 2.0 m above the PSZ. Neutron porosity values of 18–24% in the 1.0 m interval above the PSZ reflect high concentrations of water bound to clays, which outcrop-based analyses indicate are pervasive in this material (Warr and Cox, 2001).

In DFDP-1B, an ultrafine-grained, clay-rich zone was recovered in core from 128.1–128.3 m. This is underlain by 0.2 m of poorly- to moderately-cemented cataclasite that is grey-white with coarse sand-sized particles, then grey-green cataclasite, with a higher proportion of clay-sized material, then by mixtures of varying proportions of these two end members. The lowest electrical resistivity ($<80 \Omega \text{ m}$) in the borehole was encountered from 127.0 to 128.6 m (Fig. DR1). A PSZ (PSZ-1) is thus inferred to lie within the 0.5 m interval 128.1–128.6 m on the basis of extremely low resistivity (minimum $20 \Omega \text{ m}$) and high spontaneous potential (250–280 mV) values, c. 0.7 m-wide peaks in neutron porosity values (maximum 25%) and natural gamma (minimum c. 90 API), and the distinct lithology beneath (Fig. DR1). We infer the high neutron porosity of the PSZ-1 gouge to reflect a large amount of clay-bound water, based upon close inspection of the clay-rich ultrafine-grained core samples.

Footwall cataclasite

As noted above, a grey-white structureless quartz- and feldspar-rich cataclasite was sampled in DFDP-1B beneath PSZ-1. Over the next c. 15 m, this cataclasite is interlayered on a sub-meter scale with a foliated dark green cataclasite and an unfoliated grey-green cataclasite. It is not easily distinguished in hand-specimen from cemented cataclasites that immediately overlie PSZ-1. However, thin-section observations and chemical analyses suggest these rock types are not derived from typical hanging-wall protoliths.

In most of the footwall cataclasite guard resistivity is $150\text{--}200 \Omega \text{ m}$ and density logs yield a value of $2.3 \pm 0.1 \text{ g cm}^{-3}$. Spontaneous potential increases steadily downward within the unit from 190 mV to 230 mV. Geophysical logs generally have similar range and variability in both footwall and hanging-wall cataclasites. Exceptions to this are the natural gamma radiation readings (Fig. DR1A), which are notably higher in the footwall and probably indicative of higher potassium content, and the sonic logs, which show higher (by c. 0.5 km/s) V_p values above PSZ-1. The hanging-wall and footwall can be discriminated poorly on the basis of hand-specimen descriptions, but more easily from geophysical log data. A cross-plot of spontaneous potential versus resistivity illustrates progressive changes from footwall cataclasite to fault gouge, to hanging-wall cataclasite, and then hanging-wall ultramylonite (Fig. DR1C). We interpret the depth-dependent trend observed in Fig. 2C to represent the combined effects of distinct protolith chemistries with progressive comminution and alteration to clay minerals near to PSZ-1.

From 143.83–143.94 m we encountered a layer of ultrafine-grained, medium grey rock of similar texture to that comprising PSZ-1. Beneath this there is a significant lithological change to uncemented breccia of angular, cm-diameter clasts of very fine-grained dark grey-green

ultramylonite that continues to the base of the core. Wireline logs were unable to be collected across this interval due to borehole failure; nevertheless we infer this also represents a principal slip zone (PSZ-2). Our interpretation is that this deeper zone is an abandoned slip surface within the footwall (Fig. 1).

Fluid pressures, temperatures, and hydraulic observations

A series of slug tests (times for a filled borehole to drain) were conducted before and during long-term observatory installation in DFDP-1B (Bouwer, 1989; Bouwer and Rice, 1976; Hvorslev, 1951). Pressure decay was measured from the height of the water surface in the borehole (Figure DR2A). Several tests yielded permeability values in the range 1×10^{-14} m² to 6×10^{-14} , depending on assumptions used, but this is probably representative of fractured ultramylonite between depths 34 m and 53 m. There is the possibility that some fluid drained through the annulus between the rock and casing and into the sediment above, which would likely have high permeability (gravel and sand). Note that permeabilities derived from slug tests are typically higher than from laboratory samples, because permeability over a scale of 1-10 m near to a fault is mainly due to macroscopic open fractures, rather than microscopic connected pore space.

Piezometers with built-in temperature sensors were placed at depths of 72.4, 92.4, 114.9, and 136.0 m in sand packs that were hydraulically isolated by cement-bentonite grout. The decay of pressure after drilling was complete was then measured (Figure DR2B). Piezometer 1, which lies beneath the fault, was subjected to a much higher pressure anomaly during drilling, due to 0.53 MPa lower ambient fluid pressures (as determined one year later). The pressure measured by Piezometer 2 continues to decline throughout the subsequent year.

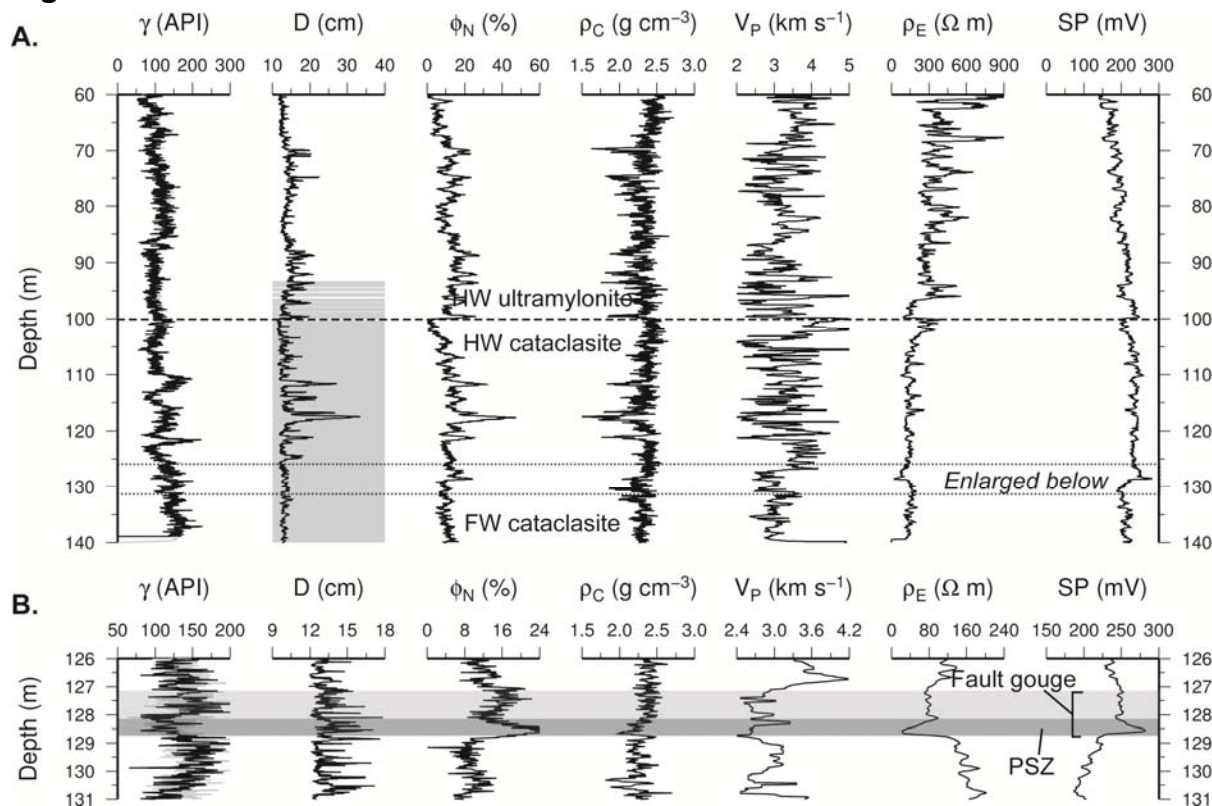
In addition to the pressure drop measured using piezometers beneath the fault in DFDP-1B, a significant pressure drop was also inferred in DFDP-1A from a sudden drain of drilling fluids into underlying gravel when the PSZ was breached. Full documentation and analysis of slug tests and pressure decay data will be presented elsewhere.

A string of resistance temperature devices (RTDs) was installed with 20 m spacing to a depth of 132.4 m. Temperature and pressure profiles obtained after one year of post-drill equilibration are shown in the main text (Fig. 2).

ACKNOWLEDGMENTS

We thank: Brent Herrick, Alan Speight, and others of Horizon Drilling; Gareth Hay of Subsurface Imaging; Alex Pyne of the Scientific Drilling Office, Victoria University of Wellington; the Department of Conservation; Te Runanga o Makaawhio; Ken and Shirley Arnold of White Heron Sanctuary Tours and the rest of the Whataroa community; Mike Hende for access; John Mead; and SIMS Pacific Metals. The project was funded by GNS Science, Victoria University of Wellington, University of Otago, University of Auckland, University of Canterbury, a grant from the Deutsche Forschungsgemeinschaft (DFG) to University of Bremen, a grant from Natural Environment Research Council (NERC – NE/H012486/1) to University of Liverpool, and the Marsden Fund of New Zealand.

Figures



c.

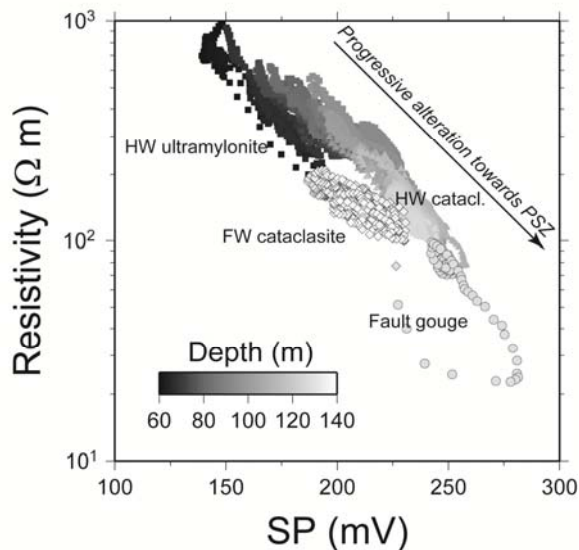


Figure DR1. Wireline geophysical data obtained in DFDP-1B.

(A) 60–140 m depth interval and (B) 126–131 m depth interval spanning the PSZ. From left to right, the curves indicate natural gamma (γ), borehole diameter (D), neutron porosity (ϕ_N), compensated density (ρ_D), P-wave velocity (V_P), short-guard electrical resistivity (ρ_E), and spontaneous potential (SP). The black and gray natural gamma curves correspond to data recorded with different logging tools. Data from shallower depths contain artefacts produced by casing and are not shown. The shading shown in the borehole diameter panel in (A) indicates where core was successfully retrieved. (C) Cross-plot between short-guard resistivity and spontaneous potential, suggesting progressively greater concentration of clay minerals near the principal slip zone, and distinct lithological differences between the fractured mylonites, hanging-wall cataclasites, fault core, and footwall cataclasites.

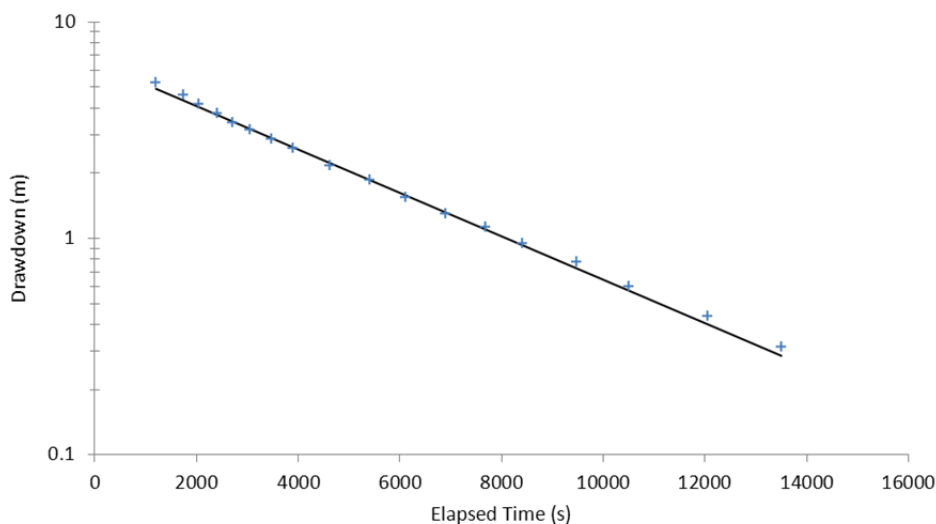
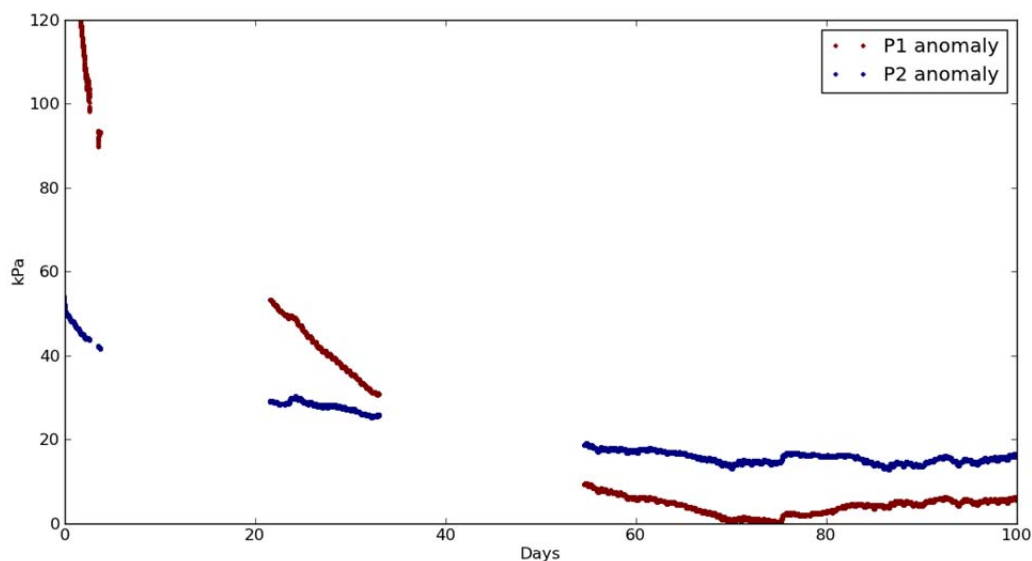
A**B**

Figure DR2. Pressure decline data from (A) slug tests; and (B) post-completion.

The straight line shown in (A) indicates the expected decline in pressure (head) for a uniform permeability of $1 \times 10^{-14} \text{ m}^2$. Pressure data shown in A represents flow out of the open DFDP-1B borehole over a depth range between 34 m (grouted casing) and 119 m, though most flow occurred between 34 m and 53 m, based upon similar results after borehole completion. Pressure data shown in (B) are from small sandpacks confined by bentonite-cement grout, and gaps in data are due to technical recording failures. Piezometer P1 is in footwall cataclasite (136.0 m); and P2 is in hanging-wall cataclasite (114.9 m). Pressure data are shown as anomalies relative to average values recorded in January 2012, one year after drilling, and have not been corrected for air pressure, earth tide, or changes in piezometric surface level.

References

- Allis, R.G., and Shi, Y., 1995, New insights to temperature and pressure beneath the central Southern Alps, New Zealand: *New Zealand Journal of Geology and Geophysics*, v. 38, p. 585–592.
- Almond, P.C., Moar, N.T., and Lian, O.B., 2001, Reinterpretation of the glacial chronology of South Westland, New Zealand: *New Zealand Journal of Geology and Geophysics*, v. 44, p. 1-15.
- Bouwer, H., 1989, The Bouwer and Rice slug test - an update: *Groundwater*, v. 27, p. 304-309.
- Bouwer, H., and Rice, R.C., 1976, Slug test for determining hydraulic conductivity of unconfined aquifers with completely or partially penetrating wells: *Water Resources Research*, v. 12, p. 423-428, doi: 10.1029/WR012i003p00423.
- Cande, S.C., and Stock, J.M., 2004, Pacific-Antarctic-Australia motion and the formation of the Macquarie Plate: *Geophysical Journal International*, v. 157, p. 399-414.
- Cooper, A.F., and Norris, R.J., 1994, Anatomy, structural evolution, and slip rate of a plate-boundary thrust: The Alpine fault at Gaunt Creek, Westland, New Zealand: *Geological Society of America Bulletin*, v. 106, p. 627–633.
- Cooper, A.F., and Norris, R.J., 2011, Inverted metamorphic sequences in Alpine fault mylonites produced by oblique shear within a plate boundary fault zone, New Zealand: *Geology*, v. 39, p. 1023-1026.
- DeMets, C., Gordon, R.G., and Argus, D.F., 2010, Geologically current plate motions: *Geophysical Journal International*, v. 181, p. 1-80, doi: 10.1111/j.1365-246X.2009.04491.x.
- Fujimoto, K., Ueda, A., Ohtani, T., Takahashi, M., Ito, H., Tanaka, H., and Boullier, A.-M., 2007, Borehole water and hydrologic model around the Nojima fault, SW Japan: *Tectonophysics*, v. 443, p. 174–182.
- Holm, D.K., Norris, R.J., and Craw, D., 1989, Brittle and ductile deformation in a zone of rapid uplift; central Southern Alps, New Zealand: *Tectonics*, v. 8, p. 153–168.
- Hvorslev, M.J., 1951, Time lag and soil permeability in ground-water observations: *Bulletin 36: Vicksburg, MS 39180-6199, USA, U.S. Army Waterways Experiment Station*, 50 p.
- Koons, P.O., 1987, Some thermal and mechanical consequences of rapid uplift; an example from the Southern Alps, New Zealand: *Earth and Planetary Science Letters*, v. 86, p. 307–319.
- Little, T.A., Cox, S., Vry, J.K., and Batt, G., 2005, Variations in exhumation level and uplift rate along the oblique-slip Alpine Fault, central Southern Alps, New Zealand: *Geological Society of America Bulletin*, v. 117, p. 707–723.
- Norris, R.J., and Cooper, A.F., 2001, Late Quaternary slip rates and slip partitioning on the Alpine Fault, New Zealand: *Journal of Structural Geology*, v. 23, p. 507–520.
- Norris, R.J., and Cooper, A.F., 2007, The Alpine Fault, New Zealand: surface geology and field relationships, *in* Okaya, D., Stern, T.A., and Davey, F., eds., *A Continental Plate Boundary: Tectonics at South Island, New Zealand: Geophysical Monograph Series, American Geophysical Union*, p. 157–175.
- Norris, R.J., Koons, P.O., and Cooper, A.F., 1990, The obliquely-convergent plate boundary in the South Island of New Zealand; implications for ancient collision zones: *Journal of Structural Geology*, v. 12, p. 715–725.

- Rhoades, D.A., and Van Dissen, R.J., 2003, Estimates of the time-varying hazard of rupture of the Alpine fault, New Zealand, allowing for uncertainties: *New Zealand Journal of Geology and Geophysics*, v. 46, p. 479–488.
- Sutherland, R., 1999, Cenozoic bending of New Zealand basement terranes and Alpine Fault displacement: A brief review: *New Zealand Journal of Geology and Geophysics*, v. 42, p. 295–301.
- Sutherland, R., Berryman, K., and Norris, R., 2006, Quaternary slip rate and geomorphology of the Alpine fault: Implications for kinematics and seismic hazard in southwest New Zealand: *Geological Society of America Bulletin*, v. 118, p. 464–474.
- Sutherland, R., Davey, F., and Beavan, J., 2000, Plate boundary deformation in South Island, New Zealand, is related to inherited lithospheric structure: *Earth and Planetary Science Letters*, v. 177, p. 141–151.
- Sutherland, R., Toy, V., Townend, J., Eccles, J., Prior, D.J., Norris, R.J., Mariani, E., Faulkner, D.R., DePascale, G., Carpenter, B.M., Boulton, C., Menzies, C.D., Cox, S., Little, T., Hasting, M., Cole-Baker, J., Langridge, R., Scott, H.R., Reid-Lindroos, Z.R., Fleming, B., and Wing, R., 2011, Operations and well completion report for boreholes DFDP-1A and DFDP-1B, Deep Fault Drilling Project, Alpine Fault, Gaunt Creek, New Zealand, GNS Science Report, Volume 2011/48: Lower Hutt, NZ, Institute of Geological & Nuclear Sciences, p. 70.
- Townend, J., Sutherland, R., and Toy, V.G., 2009, Deep Fault Drilling Project—Alpine Fault, New Zealand: *Scientific Drilling*, v. 8, p. 75–82, doi: 10.2204/iodp.sd.8.12.2009.
- Toy, V.G., Craw, D., Cooper, A.F., and Norris, R.J., 2010, Thermal regime in the central Alpine Fault Zone, New Zealand: Constraints from microstructures, biotite chemistry and fluid inclusion data: *Tectonophysics*, v. 485, p. 178–192, doi: 10.1016/j.tecto.2009.12.013.
- Toy, V.G., Prior, D.J., and Norris, R.J., 2008, Quartz fabrics in the Alpine Fault mylonites: Influence of pre-existing preferred orientations on fabric development during progressive uplift: *Journal of Structural Geology*, v. 30, p. 602–621.
- Tullis, T.E., Bürgmann, R., Cocco, M., Hirth, G., King, G.C.P., Oncken, O., Otsuji, K., Rice, J.R., Rubin, A., Segall, P., Shapiro, S.A., and Wibberly, C.A.J., 2007, Group report: rheology of fault rocks and their surroundings, *in* Handy, M.R., Hirth, G., and Hovius, N., eds., *Tectonic faults: agents of change on a dynamic earth: Dahlem Workshop Reports*: Cambridge, MA, The MIT Press, p. 183–204.
- Vandergoes, M.J., and Fitzsimons, S.J., 2003, The Last Glacial–Interglacial Transition (LGIT) in south Westland, New Zealand: paleoecological insight into mid-latitude Southern Hemisphere climate change: *Quaternary Science Reviews*, v. 22, p. 1461–1476.
- Wang, C.H., Wang, C.Y., Kuo, C.H., and Chen, W.F., 2005, Some isotopic and hydrological changes associated with the 1999 Chi-Chi earthquake, Taiwan: *Island Arc*, v. 14, p. 37–54, doi: 10.1111/j.1440-1738.2004.00456.x.
- Warr, L.N., and Cox, S., 2001, Clay mineral transformations and weakening mechanisms along the Alpine Fault, New Zealand: *Geological Society Special Publication*, v. 186, p. 85–101, doi: 10.1144/GSL.SP.2001.186.01.06.
- Zoback, M.D., Hickman, S., and Ellsworth, W., 2007, The role of fault zone drilling, *in* Schubert, G., ed., *Treatise on Geophysics*: Amsterdam, Elsevier, p. 649–674.